

Giant Dipole Resonances Built on Isobaric Analog States in Pion Double Charge Exchange

S. Mordechai,^(1,4,5) N. Auerbach,^{(2),(a)} G. R. Bureson,⁽³⁾ K. S. Dhuga,^{(3,4),(b)} M. Dwyer,⁽⁴⁾ J. A. Faucett,⁽³⁾ H. T. Fortune,⁽⁴⁾ R. Gilman,^{(4),(c)} S. J. Greene,⁽²⁾ C. Laymon,⁽⁴⁾ C. Fred Moore,⁽⁵⁾ C. L. Morris,⁽²⁾ D. S. Oakley,^{(5),(d)} M. A. Plum,⁽²⁾ S. J. Seestrom-Morris,⁽²⁾ Peter A. Seidl,^{(5),(e)} M. J. Smithson,^{(5),(f)} Z. F. Wang,^{(2),(e)} and J. D. Zumbro^{(4),(g)}

⁽¹⁾Ben-Gurion University of the Negev, Beer-Sheva 84105, Israel

⁽²⁾Los Alamos National Laboratory, Los Alamos, New Mexico 87545

⁽³⁾New Mexico State University, Las Cruces, New Mexico 88003

⁽⁴⁾University of Pennsylvania, Philadelphia, Pennsylvania 19104

⁽⁵⁾University of Texas at Austin, Austin, Texas 78712

(Received 28 September 1987; revised manuscript received 19 November 1987)

Giant resonances were observed in (π^+, π^-) double charge exchange (at $T_x=292$ MeV) on ^{56}Fe , ^{80}Se , and ^{208}Pb at excitation energies of 28.5, 34.6, and 43.6 MeV, respectively. An angular distribution for ^{56}Fe was measured and observed to have a dipole shape. The variation of excitation energy above the double isobaric analog state is consistent with an $A^{-1/3}$ dependence, as expected for giant dipole resonances built on the isobaric analog states. The ^{56}Fe angular distribution agrees well with a coupled-channels impulse-approximation calculation in which sequential single charge exchange through the isobaric analog to the giant dipole resonance is evaluated.

PACS numbers: 25.80.Fm, 24.30.Cz, 24.30.Eb, 27.40.+z

The Brink-Axel hypothesis¹ predicts the existence of collective modes of nuclear oscillations built upon excited states in nuclei. For example, it has been proposed² that each state in a nucleus has a giant dipole resonance (GDR) associated with it. These resonances will have the same features as the well-known ground-state GDR but shifted up in energy according to the energies of the excited states upon which they are built. GDR's built on states of high excitation have recently been observed in γ -ray spectra from heavy-ion fusion reactions³⁻⁶ and in proton-capture (p, γ) reactions on light nuclei at medium-energy $E_p \approx 20-80$ MeV.⁷⁻¹⁰ These studies demonstrate the existence of GDR decays populating excited final states. The results from pion single charge exchange in which giant resonances are observed should be considered as guidance when one tries to predict which of the double giant resonances will be most strongly excited in double-charge-exchange reactions. The isobaric analog state (IAS), the dipole, and also the isovector monopole resonance were all observed in (π^+, π^0) single-charge-exchange reactions¹¹⁻¹³ (with typical maximum cross sections around 0.5-1.0 mb/sr). Therefore, a combination of these resonances could, in principle, be reached in double charge exchange. However, until recently, none of these double resonances have been observed. Figure 1 shows the isovector transitions and the energies involved in exciting this new double resonance as well as the previously well-known double isobaric analog state (DIAS), which can be considered in this context as the simplest example of a double resonance.

In this Letter, we report the observation of a resolved isovector giant dipole resonance built on a discrete excited nuclear state. An "ideal" giant resonance state based

on an excited state $|n\rangle$ can be written as

$$|Q_\alpha; n\rangle = Q_\alpha |n\rangle |\langle n | Q_\alpha^\dagger Q_\alpha | n\rangle|^{-1/2} \quad (1)$$

where Q_α is a one-body operator obtained by taking a coherent sum of one-nucleon operators $q_\alpha(i)$,

$$Q_\alpha = \sum_{i=1}^A q_\alpha(i). \quad (2)$$

If $|n\rangle$ itself is a giant resonance state built on a ground state $|0\rangle$, then the state in Eq. (1) will be a double giant excitation of the type

$$|Q_\alpha; \alpha'\rangle = Q_\alpha Q_{\alpha'} |0\rangle N^{-1}, \quad (3)$$

where N^{-1} is a proper normalization factor. If the mul-

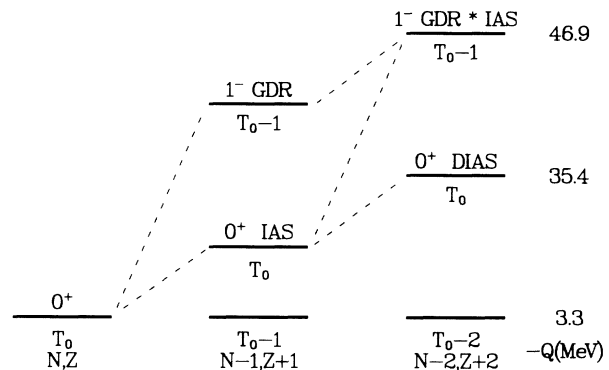


FIG. 1. Schematic energy-level diagram of analog and dipole states observed in single- and double-charge exchange. The listed Q values refer to the case of the ^{208}Pb target.

tipole isovector operators, Q_a (and Q_a'), are of the type

$$Q_{L,\mu} = \sum_{i=1}^A r_i^L Y_L(\theta_i) t_{\mu}(i), \quad (4)$$

where $\mu = +, 0,$ or $-$, then by taking $\mu = -$ and $L = 0$ and 1 we may write the model state as

$$|D_{-}; A\rangle = \sum_{i=1}^A r_i Y_1(\theta_i) t_{-}(i) |A\rangle N^{-1}, \quad (5)$$

where

$$|A\rangle = \sum_{i=1}^A t_{-}(i) |0\rangle (N-Z)^{-1/2} \quad (6)$$

is the isobaric analog state, and the operator t_{-} is the isospin-lowering operator that changes a neutron into a proton. Equation (5) describes the $\Delta T_z = -2$ component of a dipole built on the isobaric analog state. We label this state as $GDR \otimes IAS$ in Fig. 1. It is this state that we consider here.

The measurements were performed with the energetic pion channel and spectrometer (EPICS) at the Clinton P. Anderson Meson Physics Facility (LAMPF) with the standard pion double-charge-exchange setup.¹⁴ Earlier papers reported cross sections for the (π^+, π^-) reaction on ^{56}Fe ,¹⁵⁻¹⁷ ^{80}Se ,¹⁸ and ^{208}Pb ¹⁹ at an incident pion en-

ergy $T_{\pi} = 292$ MeV. The isotopic purity and areal density of the targets used in the present measurements are 91.8%, 1.199 g/cm² for ^{56}Fe ; 49.8%, 1.86 g/cm² for ^{80}Se ; and >99%, 0.516 g/cm² for ^{208}Pb .

Figure 2 shows the ^{56}Fe missing-mass spectra at two angles. In addition to the DIAS, both spectra show the existence of a relatively wider peak located in the continuum region at about 18.6 MeV above the DIAS. These bumps are labeled GR in the figure. Cross sections were extracted for the DIAS and GR with the code NEWFIT written by one of us (C.L.M.). The spectra have been corrected for the measured variation of the spectrometer acceptance as a function of momentum. The peaks were fitted with a Gaussian shape of variable width. The background (dashed lines), which arises from double-charge-exchange cross section to discrete low-lying states and the continuum, was fitted with a three-parameter exponential shape of the form $R_1 + R_2 \exp(E/R_3)$. The solid lines are the resulting fit to the spectra.

Figure 3 presents the angular distribution extracted for the GR on ^{56}Fe at $T_{\pi} = 292$ MeV. The maximum cross section was observed at 10° – 15° , with a slightly smaller cross section at 5° . At a scattering angle of 25° the GR peak is very weak and can hardly be observed.

A calculation has been performed for the GR with use of a pion coupled-channels impulse-approximation code (CCIA) NEWCHOP.²⁰ The coupled-channels calculations included the ground state, the IAS, the GDR, and the $GDR \otimes IAS$ (see Fig. 1). The collective model has

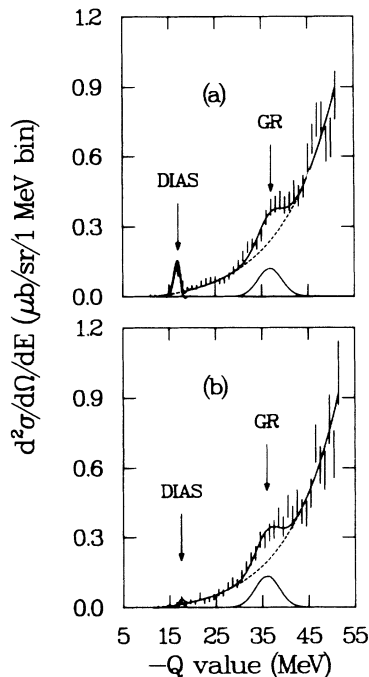


FIG. 2. Double-differential cross-section spectrum for (π^+, π^-) reaction on a ^{nat}Fe target at $T_{\pi} = 292$ MeV: (a) $\theta_{\text{lab}} = 5^{\circ}$ and (b) $\theta_{\text{lab}} = 15^{\circ}$. The arrows indicate the fitted location of the DIAS and the giant resonance (GR). Short vertical lines represent the statistical uncertainty of the data. The dashed line is the fitted background with an exponential shape and the solid line is the fit to the spectrum with use of NEWFIT.

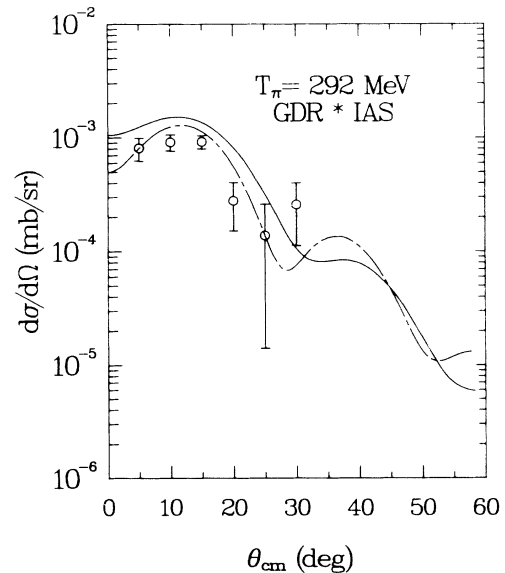


FIG. 3. Angular distribution for the peak labeled GR in the double-charge-exchange spectrum on ^{56}Fe shown in Fig. 2. The cross sections have been extracted with use of a Gaussian line shape for the giant resonance with a constant width of 6.0 MeV and constant $E_x = 28.5$ MeV. The solid and dot-dashed lines are CCIA calculations with use of volume and surface transition densities, respectively.

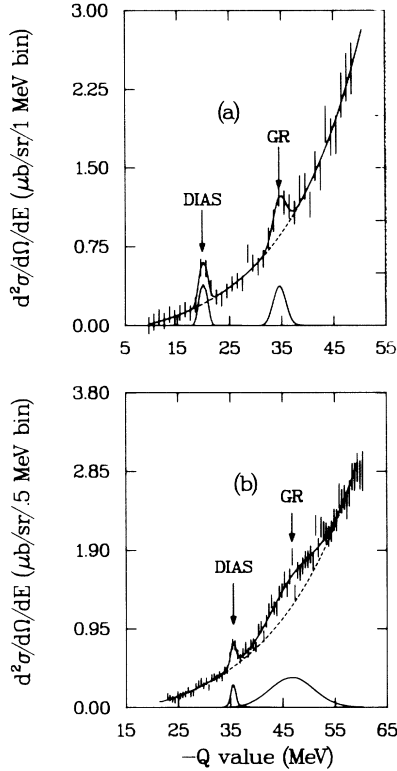


FIG. 4. (a) Same as Fig. 2(a) but for a ^{nat}Se target. The DIAS and the GR peaks thus contain contributions from several isotopes. The spectrum is binned in 1.0-MeV bin size. (b) Same as above but for enriched ^{208}Pb target and a bin size of 0.5 MeV.

been used to obtain the radial shape of the transition density for the dipole. For the transition to the isobaric analog state we used two different transition densities—one volume peaked and one surface peaked. The strengths of each single charge exchange have been separately adjusted to reproduce the experimental or extrapolated (π^+ , π^0) cross section of the GDR \otimes IAS¹³ and IAS.^{21,22}

Details on these calculations will be reported elsewhere.²³ The calculated cross section for the GDR \otimes IAS (see Fig. 3) is found to peak near 11° (c.m.) for ^{56}Fe . This is an expected result for coupling of a monopole transition (which peaks at 0°) with a dipole transition (which peaks around 11°). The calculated curves with both IAS transition densities predict the shape of the angular distribution without any additional normalization. Therefore the angular-distribution measurement on ^{56}Fe gives strong support for the identification of this resonance as a giant dipole built on the isobaric analog state (or equivalently, as the isobaric analog of the charge-exchange giant dipole).

Figure 4 displays spectra obtained at 5° double charge exchange on ^{nat}Se and ^{208}Pb targets. Again, both the DIAS and a higher-lying peak are apparent in both targets. Table I summarizes the deduced excitation energies, widths, and cross sections for the DIAS and the giant resonances from the Gaussian fits. The excitation energies of the GR above the DIAS are best fitted with an $A^{-1/3}$ dependence (times a normalization factor of 68 ± 2) which supports the interpretation of these peaks as giant-dipole oscillations built on the isobaric analog as an intermediate state. It is for this reason that we refer to these states as GDR \otimes IAS. The measured cross section for this state at $T_\pi = 292$ MeV and $\theta_{lab} = 5^\circ$ (Table I) increases by about a factor of 11 from ^{56}Fe to ^{208}Pb . We also note that for all three nuclei the cross section for the GDR \otimes IAS is larger than the DIAS cross section. The ratio $\sigma(\text{GDR}\otimes\text{IAS})/\sigma(\text{DIAS})$ is 3.4, 2.4, and 9.4 for ^{56}Fe , ^{80}Se , and ^{208}Pb , respectively. If we denote the target-nucleus ground-state T_z by T_0 , then the GDR \otimes IAS can have in general $T = T_0 \pm 1$ or T_0 ; from isospin arguments the lowest- T component is the strongest. This state with $T_0 - 1$ is the analog of the dipole observed in single-charge-exchange (π^+ , π^0) scattering, as illustrated in Fig. 1. The measured width for the GDR \otimes IAS on ^{56}Fe ($\Gamma = 6.0$ MeV) is comparable with the widths of the charge-exchange GDR on ^{40}Ca , ^{60}Ni ,

TABLE I. Results from the double-charge-exchange reaction on ^{56}Fe , ^{nat}Se , and ^{208}Pb targets at an incident pion energy $T_\pi = 292$ MeV and $\theta_{lab} = 5^\circ$ compared with theoretical CCIA calculations.

Target	E_x (DIAS) (MeV)	$(d\sigma/d\Omega)$ (DIAS) ($\mu\text{b}/\text{sr}$)	E_x (GR) (MeV)	δE_x^a (MeV)	Γ (GR) (MeV)	Expt. $(d\sigma/d\Omega)$ (GR) ^b ($\mu\text{b}/\text{sr}$)	CCIA $(d\sigma/d\Omega)$ (GR) ^c ($\mu\text{b}/\text{sr}$)
^{56}Fe	9.90 ± 0.05	0.24 ± 0.05	28.52 ± 0.55	18.62 ± 0.60	6.0 ± 1.8	0.81 ± 0.19	1.24
^{80}Se	19.99 ± 0.10	0.92 ± 0.14^d	34.62 ± 0.56	14.63 ± 0.66	4.1 ± 2.2	2.21 ± 0.44	2.97
^{208}Pb	32.13 ± 0.12	0.96 ± 0.19	43.63 ± 0.78	11.17 ± 0.90	11.0 ± 1.9	9.00 ± 0.80	9.72

^a $\delta E_x = E_x(\text{GR}) - E_x(\text{DIAS})$.

^b Experimental cross section for GDR \otimes IAS at 5° from the present measurements.

^c Calculated cross sections for the dipole IAS with use of the code NEWCHOP (Ref. 20) at 5° and $T_\pi = 292$ MeV.

^d The yield in the DIAS from ^{nat}Se includes contributions from all naturally occurring Se isotopes, since they have about the same Q value. The listed cross section represents an average DIAS cross section. However, based on the isotopic purity of the ^{nat}Se target and the assumption that the DIAS cross section at 5° scales like $(d\sigma/d\Omega)(\text{DIAS}) = \frac{1}{2}(N-Z)(N-Z-1)A^{-10/3}$, about 60% of the yield in the DIAS peak arises from ^{80}Se . The DIAS cross section for ^{80}Se is therefore approximately $0.92 \times (0.60/0.498) = 1.11 \mu\text{b}/\text{sr}$.

and ^{90}Zr .¹³ This width gives a better fit to the data at forward angles ($5^\circ \rightarrow 15^\circ$) where the peak clearly stands above background. We note, however, that it is difficult to make a clear determination of the width in this case since the data show a hint of a weaker bump just above the one labeled GR (Fig. 2). Fitting the whole region with a single peak of unconstrained width gives a width of about 10 MeV. In ^{56}Fe , T_0 is small (viz. 2) and therefore the strength of the isospin members may be such that we are observing more than one member of the GDR \otimes IAS. For ^{208}Pb the width of the GR is about 11.0 MeV, which is larger than the approximate width of 6 MeV reported for the analog dipole in the reaction $^{208}\text{Pb}(\pi^+, \pi^0)$.¹³ A relatively small width of about 4.1 MeV was observed in the $^{\text{nat}}\text{Se}$ target. The calculated CCIA cross sections for the GDR \otimes IAS at $T_\pi = 292$ MeV are listed in Table I. The calculations give a good account of the measured cross section in all three cases and predict very well the increase in the cross section with A . Theoretical work on some of the properties of the dipole IAS, double dipole, and other types of giant resonances built on excited states is now in progress.²⁴

In conclusion, we have reported the first observation of charge-exchange giant dipole resonances built on the isobaric analog states in pion double-charge-exchange scattering on ^{56}Fe , ^{80}Se , and ^{208}Pb . These results show that the study of exotic resonances such as the double giant dipole in double-charge-exchange reactions is quite promising. CCIA calculations with collective transition densities give a quantitatively correct description of the three measured cross sections and of the angular distribution shape for ^{56}Fe .

We thank David Bowman, Dan Strottman, and Benjamin Zeidman for helpful comments and useful discussion. This work was supported in part by the U.S. Department of Energy, the Robert A. Welch Foundation, and the National Science Foundation.

^(a)Permanent address: Tel-Aviv University, Tel-Aviv, Israel.

^(b)Permanent address: George Washington University,

Washington, D.C. 20052.

^(c)Present address: Argonne National Laboratory, Argonne, IL 60439.

^(d)Present address: University of Colorado, Boulder, CO 80309.

^(e)Present address: Lawrence Berkeley Laboratory, Berkeley, CA 94720.

^(f)Present address: Daresbury Laboratory, Daresbury, Warrington WA 4DD, United Kingdom.

^(g)Present address: Los Alamos National Laboratory, Los Alamos, NM 87545.

¹D. M. Brink, Ph.D. thesis, University of Oxford, 1955 (unpublished); P. Axel, *Phys. Rev.* **126**, 671 (1962).

²G. F. Bertsch and R. A. Broglia, *Phys. Today* **39**, No. 8, 44 (1986).

³J. O. Newton *et al.*, *Phys. Rev. Lett.* **46**, 1383 (1981).

⁴A. M. Sandorfi *et al.*, *Phys. Lett.* **130B**, 19 (1983).

⁵J. J. Gaardhøje *et al.*, *Phys. Rev. Lett.* **56**, 1783 (1986).

⁶C. A. Gossett *et al.*, *Phys. Rev. Lett.* **54**, 1486 (1985).

⁷M. A. Kovash *et al.*, *Phys. Rev. Lett.* **42**, 700 (1979).

⁸H. R. Weller *et al.*, *Phys. Rev. C* **25**, 2921 (1982).

⁹D. H. Dowell *et al.*, *Phys. Rev. Lett.* **50**, 1191 (1983).

¹⁰Kurt A. Snover, *Annu. Rev. Nucl. Part. Sci.*, **36**, 545 (1986), and references therein.

¹¹J. D. Bowman *et al.*, *Phys. Rev. Lett.* **50**, 1195 (1983).

¹²F. Irom *et al.*, *Phys. Rev. C* **34**, 2231 (1986).

¹³A. Erell *et al.*, *Phys. Rev. C* **34**, 1822 (1986).

¹⁴H. A. Thiessen *et al.*, Los Alamos Scientific Laboratory Report No. LA-6663-MS, 1977 (unpublished); S. J. Greene *et al.*, *Phys. Lett.* **88B**, 62 (1979).

¹⁵Peter A. Seidl *et al.*, *Phys. Rev. Lett.* **50**, 1106 (1983).

¹⁶H. T. Fortune *et al.*, *Phys. Rev. C* **35**, 1151 (1987).

¹⁷J. D. Zumbro *et al.*, *Phys. Rev. C* **36**, 1479 (1987); R. Gilman *et al.*, to be published.

¹⁸R. Gilman *et al.*, *Phys. Rev. C* **35**, 1334 (1987).

¹⁹C. L. Morris *et al.*, *Phys. Rev. Lett.* **54**, 775 (1985).

²⁰E. Rost, computer code CHOPIN (unpublished). The code has been modified by one of us (C.L.M.) to calculate pion charge-exchange reactions and renamed NEWCHOP.

²¹Helmut W. Baer, in *Proceedings of the International Symposium on Nuclear Spectroscopy and Nuclear Reactions, Osaka, Japan, 1984*, edited by H. Ejiri and T. Fukuda (World Scientific, Singapore, 1984).

²²U. Sennhauser *et al.*, *Phys. Rev. Lett.* **51**, 1324 (1983).

²³S. Mordechai *et al.*, to be published.

²⁴N. Auerbach *et al.*, to be published.